

# Effect of Carrier Ionic Strength in Microscale Cyclical Electrical Field-Flow Fractionation

Ameya S. Kantak, Merugu Srinivas, and Bruce K. Gale\*

Department of Mechanical Engineering, University of Utah, 50 South Central Campus Drive, MEB Room 2110, Salt Lake City, Utah 84112-9202

Recent work with cyclical electrical field-flow fractionation systems has shown promise for the technique as a separation and analysis tool, but little is understood about how the carrier composition in the system affects its capabilities. The electrical properties of microscale CyEIFFF systems change when the carrier ionic conditions are altered, and it is well known that the effects of increasing ionic strength carriers on retention in normal EIFFF systems are severe. Specifically, retention levels fall significantly. Accordingly, this work seeks to understand the effect that increasing carrier ionic strength in CyEIFFF has on nanoparticle retention in the channels. The retention of polystyrene particles in the CyEIFFF microsystem is reported at various ionic strengths of ammonium carbonate and at a variety of pH levels. The experiments are compared to the theory of CyEIFFF available in the literature. The results indicate that the ionic strength of the carrier has a significant impact on retention and that high ionic strength carrier solutions lead to poor performance of the CyEIFFF system. These results have significant impact on the possible uses of the technique and its applications, especially in the biomedical arena.

Cyclical electrical field-flow fractionation (CyEIFFF) employs alternating/cyclical fields to generate separation based on differential electrophoretic mobilities and has recently been demonstrated as a technique for the characterization of colloids and nanoparticles.<sup>1</sup> The impetus for development of the technique was the advent of microscale field-flow fractionation (FFF) systems,<sup>2–6</sup> which seemed to have the proper electrical properties for the use of cyclical fields. Indeed, the electrical properties have been shown to be a critical factor in the performance of CyEIFFF systems.<sup>7,8</sup> The carrier solution in the FFF channel is known to play a significant role in determining the electrical properties of an EIFFF channel under dc operation,<sup>9,10</sup> and the carrier solution is expected

to play an equally important role in CyEIFFF. Since the role the carrier electrical properties play in CyEIFFF is not well understood, the primary purpose of this work is to determine the effect of the carrier properties on the effective electric fields in an EIFFF channel and the subsequent retention of particles. In this work, we explore the performance of a CyEIFFF microsystem under a range of ionic conditions by monitoring the retention of nanoparticles for the various conditions. We rely heavily on theoretical mathematical models developed previously<sup>7,11,12</sup> to explain various phenomena observed in the system, but also present some of the limitations of these models as well as suggestions to improve the model predictions.

## THEORY

CyEIFFF theory is becoming well developed in the literature<sup>7,11,12</sup> and is used in this paper for comparison with the experimental data, and the reader is referred there for details. Only important details are provided here.

A CyEIFFF system is essentially the same as a traditional EIFFF system with two planar electrodes separated by a thin spacer defining a microchannel. The flow in the channel is laminar, which necessitates that a parabolic flow velocity profile be present. An oscillating electrical field is provided across the flow channel, such that particles susceptible to the electrical field move in a manner similar to that shown in Figure 1. In CyEIFFF, depending upon the extent of oscillation of the particles in the channel, the mode of operation is defined. A dimensionless parameter  $\lambda_o$ , representing the ratio of the maximum travel of a particle into the channel and the electrode separation distance, is used to describe the motion of particles, which for a square waveform is given by

$$\lambda_o = \mu E_{\text{eff}}/2fw = \mu V_B/2fw^2 \quad (1)$$

where  $\mu$  is the particle electrophoretic mobility,  $f$  is the frequency,  $E_{\text{eff}}$  is the effective field in the bulk,  $V_B$  is the potential drop across the carrier solution in the channel, and  $w$  is the electrode separation distance. If  $\lambda_o < 1$ , the particle cannot reach the opposite wall, and is said to be in mode I. If  $\lambda_o > 1$ , the particle does reach the opposite wall and is said to be in mode III. Mode

\* To whom correspondence should be addressed. Phone: (801) 585-5944. Fax: (801) 585-9826. E-mail: gale@mech.utah.edu.

(1) Merugu, S.; Gale, B. K. *Electrophoresis* 2005, 26, 9, 1623–1632.

(2) Giddings, J. C. *J. Microcolumn Sep.* 1993, 5, 497–503.

(3) Gale, B. K.; Caldwell, K. D.; Frazier, A. B. *IEEE-TBE* 1998, 45 (12), 1459–1469.

(4) Lao, A. I. K.; Trau, D.; Hsing, I. M. *Anal. Chem.* 2002, 74, 5364–5369.

(5) Gale, B. K.; Caldwell, K. D.; Frazier, A. B. *Anal. Chem.* 2002, 74, 1024–1030

(6) Edwards, T. L.; Gale, B. K.; Frazier, A. B. *Proc. Transducers '99* 1999, 742–745.

(7) Kantak, A. S.; Merugu, S.; Gale, B. K. *Electrophoresis*. In press.

(8) Kantak, A. S.; Merugu, S.; Gale, B. K. Submitted to *Lab Chip*.

(9) Palkar, S. A.; Schure, M. R. *Anal. Chem.* 1997, 69 (16), 3223–3229.

(10) Palkar, S. A.; Schure, M. R. *Anal. Chem.* 1997, 69 (16), 3230–3238.

(11) Giddings, J. C. *Anal. Chem.* 1986, 58, 2052–2056.

(12) Lee, S.; Myers, M. N.; Beckett, R.; Giddings, J. C. *Anal. Chem.* 1988, 60, 1129–1135.

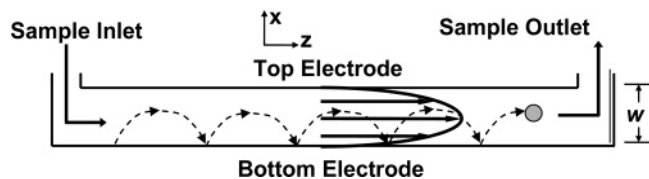


**Figure 1.** Typical CyEIFFF system cross section.

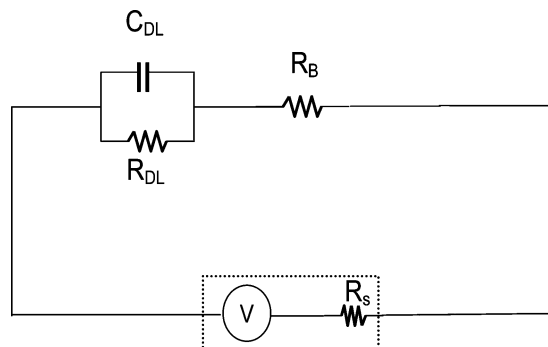


**Figure 2.** Modified equivalent circuit showing the source resistance,  $R_s$ . The source resistance modifies the voltage division among the circuit components.

II is where the particle has a grazing incidence at either of the walls with  $\lambda_0 = 1$ .

In FFF, the retention ratio  $R$  is defined by

$$R = t_0/t_r \quad (2)$$

where  $t_0$  is the experimental elution time of an unretained particle and  $t_r$  is the elution time of a retained particle and can be related to  $\lambda_0$  depending on the mode of operation.  $R$  in mode I is given by

$$R = 3\lambda_0(1 - 2\lambda_0/3) \quad \text{for } \lambda_0 \leq 1 \quad (3)$$

whereas,  $R$  in mode III is given by

$$R = 1/\lambda_0 \quad \text{for } \lambda_0 \geq 1 \quad (4)$$

At  $\lambda_0 = 1$ , eqs 3 and 4 connect to create a continuous function, so mode II can be represented by either model. The value of  $R$  equal to unity corresponds to  $\lambda_0 = 1$ . However, this unity value is not the maximum value of  $R$ . The maximum value of  $R$  is 1.125, which corresponds to  $\lambda_0 = 0.75$ .<sup>11</sup>

The effective field acting on particles in the channel can be challenging to determine, as it is a complex function of the carrier properties, the electrode material, the frequency and magnitude of the applied voltage, and the particle properties. To simplify the determination of  $E_{\text{eff}}$ , a lumped electrical parameter model has been developed that accounts for these various effects.<sup>7</sup> The equivalent electrical circuit for the EIFFF channel is shown in Figure 2 including the capacitance,  $C_{\text{DL}}$ , and resistance,  $R_{\text{DL}}$ , of both electrical double layers at the electrode-carrier interface, and the resistance of the bulk of the carrier,  $R_B$ , and the source resistance,  $R_s$ . All these lumped electrical parameter values (except the source resistance) change depending on the ionic strength of the carrier solution. The effective electric field  $E_{\text{eff}}$  available to

influence particles in the channel is given by<sup>7,8</sup>

$$E_{\text{eff}} = \frac{VR_B}{w} \sqrt{\frac{1 + (2\pi f R_{\text{DL}} C_{\text{DL}})^2}{(R_B + R_s + R_{\text{DL}})^2 + (2\pi f (R_B + R_s) R_{\text{DL}} C_{\text{DL}})^2}} \quad (5)$$

where  $V$  is the applied voltage. The electrical time constant of the CyEIFFF system  $\tau$  is given by

$$\tau = \frac{(R_B + R_s) R_{\text{DL}} C_{\text{DL}}}{R_B + R_s + R_{\text{DL}}} \quad (6)$$

One can observe that the bulk voltage is dependent upon the frequency and magnitude of the applied voltage as well as the electrical circuit parameters of the system and, thus, on the properties of the carrier solution.

Not only do the frequency and the magnitude of applied voltage play an important role in deciding the particle motion and the mode of operation in CyEIFFF, but the electrophoretic mobility of the particles in the channel is also critical. The electrophoretic mobility of the particle depends on the ionic strength of the carrier solution; this modifying relationship is given by Oshima as<sup>13</sup>

$$\mu = \frac{2\epsilon_0\epsilon_r\zeta}{3\eta} \left( 1 + \frac{1}{2 \left[ 1 + \frac{2.5}{\kappa a} (1 + 2e^{-\kappa a}) \right]^3} \right) \quad (7)$$

where  $\kappa$  is the inverse Debye length of the particle double layer,  $\epsilon_0$  is the permittivity of free space (vacuum), and  $\epsilon_r$  is the relative permittivity,  $\zeta$  is the zeta potential of the particle,  $a$  is particle radius, and  $\eta$  is the viscosity of the carrier. The particle mobility is close to 70% (of its high ionic strength value) for low ionic strength carriers (ultrapure DI water or the low micromolar range), and it is over 90% of its maximum value for carriers with an ionic strength above 1.0 mM. Thus, at a minimum, retention times are expected to vary for nanoparticles being retained in a CyEIFFF channel based on changes in mobility with carrier ionic properties. Therefore, in the simulations included in this work, the changes in mobility values due to varying ionic strength are included to determine their significance.

To determine the extent of peak broadening under various ionic strength conditions, the concept of plate heights from chromatography may be used as the measure of broadening. In plate theory, the length  $L$  of a separation column can be broken into  $N$  theoretical plates of height  $H$ , given by

$$H = L/N \quad (8)$$

where  $N$  is calculated using<sup>14</sup>

$$N = 5.55(A/w_{1/2})^2 \quad (9)$$

where  $A$  is the location of the center of the elution peak along the  $x$ -axis and  $w_{1/2}$  is the width of the particle elution peak at half

(13) Lyklema, J. *Fundamentals of Interface and Colloid Science: Vol. II: Solid-Liquid Interfaces*; Academic Press Inc.: San Diego, 1995.

of the peak height. From elution profiles, total plate heights  $H$  can be measured experimentally. The higher the plate height, the greater the extent of peak broadening. We have used this concept of plate heights to emphasize the role of peak broadening only and warn the reader to interpret them in the context of peak broadening only.

## EXPERIMENTAL METHODOLOGY

For the experimental efforts, an EIFFF microsystem with graphite electrodes was fabricated using methods described previously<sup>7</sup> and was 5.1 cm long, 30  $\mu\text{m}$  deep, and 5 mm wide. The same system dimensions were used to generate simulated data from CyEIFFF theory<sup>11</sup> and the lumped electrical parameter model for effective fields.<sup>7</sup> Aminated 100-nm polystyrene (PS) nanoparticles having electrophoretic mobility of  $2.57 \times 10^{-4} \text{ cm}^2/(\text{V}\cdot\text{s})$  were chosen as representative particles for these experiments, because of their known retention properties and characteristics in CyEIFFF systems. Also, for particles above  $\sim 500$  nm, steric effects can become an important issue,<sup>5</sup> and smaller size particles (such as 10–50 nm) are prone to diffusion; simulations<sup>7</sup> show that diffusion effects are reasonably small for 100-nm particles. Therefore, 100-nm particles were chosen since they avoided these two additional complications. The particle mobility was adjusted using eq 7 at various carrier ionic strengths. The experimental setup included the following: a dc power supply (Agilent, model E3630A), an ac function generator (Hewlett-Packard, model HP 33120A), a multimeter (Hewlett-Packard, model HP 34401A), a data acquisition setup (LabVIEW, National Instruments), and a UV/visible absorbance detector (ESA, model 520) and is exactly the same as described previously.<sup>7,8</sup> The carrier flow was controlled using a syringe pump (KD Scientific), and the nanoparticle samples were injected using a Hamilton microliter syringe. The output provided by the UV/visible absorbance detector was acquired by a data acquisition system associated with a computer and LabVIEW software.

The lumped electrical parameters of the equivalent circuit were measured using standard step voltage experiments.<sup>7</sup> To check the effect of source resistance on the applied voltage distribution in the electric circuit including the microsystem and power source, a very small resistance ( $\sim 10 \Omega$ ) was added in series with the microsystem, the voltage drop across it was measured, and then the voltage drop across the microsystem was back-calculated.

The carriers used in the experiments were ultrapure DI water (resistivity 18.2  $\text{M}\Omega\cdot\text{cm}$ ) (EasyPure, Barnstead) and solutions of ammonium carbonate with ionic strengths up to 5.0 mM in air-equilibrated DI water and ultrapure DI water. The pH was adjusted using potassium hydroxide and hydrochloric acid solutions. The conductivity values were measured using a conductivity meter (Control Co., Inc.), and pH values were recorded using a pH meter (Orion pH and pH/ion meter, Orion 250A) with calibrations using standard solutions (NIST certified). The readings of pH and conductivity were taken immediately before and after all experiments.

Characterization experiments were performed with PS particle standards (Polysciences, Inc.) at a concentration of 0.01 wt % and a sample volume of 0.2  $\mu\text{L}$ /injection. Sample relaxation was

performed in some experiments by stopping the carrier flow for a short time period<sup>8</sup> in order to reduce the peak broadening and allow the particles to start their motion near one of the walls. The electrophoretic mobilities ranged from  $2.0 \times 10^{-4}$  to  $3.0 \times 10^{-4} \text{ cm}^2/(\text{V}\cdot\text{s})$  as measured using a zeta potential analyzer (Brookhaven Instruments Zeta Plus). The particles were detected at 225 nm on a UV/visible absorbance detector model 520 (ESA Inc.) with a flow cell volume of 1.2  $\mu\text{L}$ . Flow rates were maintained at 1.0 mL/h. The applied voltage was either 3.0 V peak to peak (VPP) or 5.0 VPP. In another set of experiments, the pH values were adjusted by the addition of a potassium hydroxide and hydrochloric acid in air-equilibrated DI water. The overall addition is essentially potassium chloride with hydrogen and hydroxyl ions. Potassium chloride is an indifferent electrolyte at low concentrations (less than 1.0 mM) in that it is not involved in electrode reactions and it affects only the charge transport processes in the bulk phase of the carrier.<sup>9</sup> Therefore, such additions typically do not alter electrode reactions. These experiments were performed with an ionic strength of 50  $\mu\text{M}$  ammonium carbonate in air-equilibrated DI water.

To obtain a general understanding of the effect of carrier conditions on the extent of peak broadening in CyEIFFF systems, and thus on potential resolution, plate heights were measured as a function of operating conditions and carrier ionic strength. Peak broadening, which leads to increased plate heights, is an undesirable event in chromatographic systems since it decreases the resolution and overall performance of the system. Little data are available for plate heights in FFF systems. Plate heights were calculated using eqs 8 and 9 from the plate theory of chromatography<sup>15</sup> and experimentally generated fractograms from the characterization experiments. Operation of the CyEIFFF channel was assumed to be linear.

The absolute sample recovery experiments in this work<sup>16</sup> showed that  $\sim 87$ – $94\%$  of the injected samples were recovered in most experiments. The peak average values were calculated by taking area moments for every elution profile using Microsoft Excel and Peakfit (SyStat). With most of the injected particle mass recovered during the experiments, it was reasonable to assume that plate theory could be applied. From the particle elution profiles, average elution time values were determined by taking the area moments<sup>3,5,14</sup> of the eluted peaks. Run orders were randomized to reduce user and instrumental biases. The elution data were reported within 95% confidence interval, and the standard deviations in reported elution times were  $\pm 3$  s. The errors and uncertainties reported in various measurements of elution times were  $\sim 7.28\%$ .

## RESULTS AND DISCUSSION

**Electrical Parameters.** The measured lumped electrical parameter values  $R_{\text{DL}}$ ,  $C_{\text{DL}}$ , and  $R_{\text{B}}$  (for the electrical double layer model) from the time constant and electrical property measurement experiments are listed in Table 1. The CyEIFFF system electrical time constants for a range of applied frequencies using air-equilibrated DI water-based solutions of ammonium carbonate

(14) Said, A. S. *Theory and Mathematics of Chromatography*; Dr. Alfred Huethig Publishers: Heidelberg, Germany, 1981.

(15) Ladisch, M. R. *Bioseparations engineering: Principles, practice and economics*; John Wiley & Sons: New York, 2001.

(16) Ratanathanawongs-Williams, S. K.; Giddings, J. C. Sample Recovery. In *Field-flow fractionation handbook*; Schimpf, M., Caldwell, K., Giddings, J. C., Eds.; John Wiley and Sons Inc.: New York, 2000.

**Table 1. CyEIFF Graphite Microsystem Electrical Properties for Different Ionic Strength Carriers (Source Resistance 60  $\Omega$ )**

$f$ (Hz)	$R_B$ ( $\Omega$ )	$R_{DL}$ ( $\Omega$ )	$C_{DL}$ (F)
Carrier: 5 $\mu$ M $(\text{NH}_4)_2\text{CO}_3$			
1	740	5217	$5.77 \times 10^{-6}$
5	740	2356	$5.50 \times 10^{-6}$
10	740	2343	$5.16 \times 10^{-6}$
50	740	1358	$3.66 \times 10^{-6}$
Carrier: 100 $\mu$ M $(\text{NH}_4)_2\text{CO}_3$			
1	595	4434	$1.1 \times 10^{-5}$
5	595	1866	$1.02 \times 10^{-5}$
10	595	1135	$8.6 \times 10^{-6}$
50	595	640	$8.3 \times 10^{-6}$
Carrier: 500 $\mu$ M $(\text{NH}_4)_2\text{CO}_3$			
1	75	3972	$8.06 \times 10^{-5}$
5	75	1347	$7.69 \times 10^{-5}$
10	75	811	$6.66 \times 10^{-5}$
50	75	486	$5.23 \times 10^{-5}$

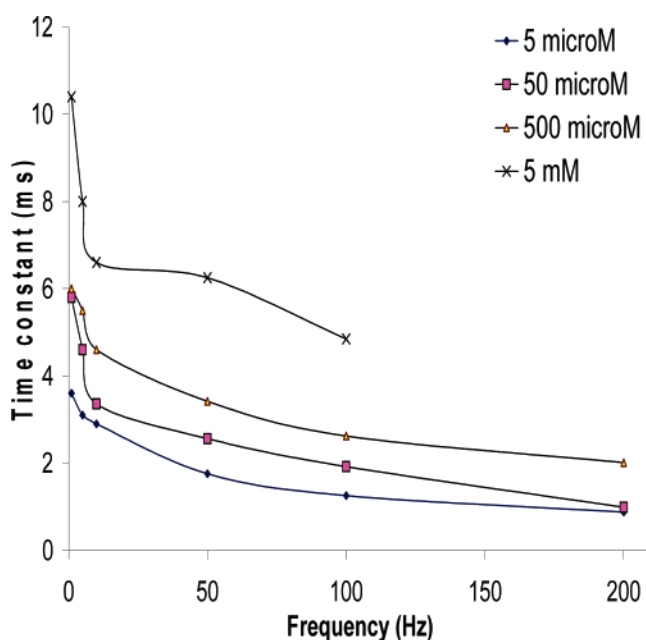


**Figure 3.** Time constants of the microsystem at various frequencies and at various ionic strengths of ammonium carbonate in DI water. The flow rate was set at 1.0 mL/h, and voltage was 2.0 VPP.

at various ionic strengths are shown in Figure 3. The variation in time constant with frequency and carrier composition clearly shows that the microsystem cannot be assumed as a linear and

**Table 3. Measured Conductivity Values for Various Carrier Ionic Strengths**

carrier type	conductivity ( $\mu\Omega/\text{cm}$ )	bulk resistance $R_B$ ( $\Omega$ )
ultrapure DI	1.05	880.20
100 $\mu$ M	2.66	595.48
0.5 mM	11.40	75.50
0.7 mM	42.00	31.80
1.0 mM	74.00	17.40
3.0 mM	123.06	9.56
5.0 mM	176.38	6.67

ideal capacitor as assumed previously.<sup>7,8</sup> Despite this assumption, the results predicted using a lumped electrical parameter model<sup>7</sup> showed reasonably good agreement with the experimental data using low ionic strength carriers. However, in this work, it was found that the values of  $R_{DL}$  and  $C_{DL}$  are not constant for a given instrument due to their dependence on carrier composition and the applied frequency, but this does not necessarily indicate that an assumption of constant values is unreasonable unless large variations in carrier ionic strength or frequency are used. Clearly from Table 1 and Figure 3,  $R_{DL}$  and  $C_{DL}$  are highly dependent on operating conditions rather than constant values, and this fact must not be ignored when computing theoretical elution times and making analytical measurements. In the calculations of Table 1, it is assumed that bulk resistance  $R_B$  values remain constant, which is a reasonable assumption since changes in bulk resistance are not expected unless much higher frequencies are used (MHz).

From Table 2 for any given ionic strength, with increasing frequency, the voltage across the microsystem was shown to decrease, which does not mean that the voltage across the bulk carrier in the channel has decreased. Briefly, the overall voltage drop across the microsystem decreases, since bulk resistance is constant and impedance of the EDL decreases. but the overall voltage drop across the bulk of the channel increases as the voltage distribution between components changes.<sup>7,8,17</sup> Specifically, the drop across the source resistance increases. In fact, the source resistance becomes even more important in the event of higher ionic strengths as seen from Table 2 and Table 3. The  $R_B$  values decrease with increasing ionic strengths indicating that the conductivity of the carrier has increased in the bulk, which causes the voltage drop across the bulk of the channel to fall (Table 2) with increasing ionic strengths, since more of the voltage is now dropped across the source resistance and the double layer. Thus, the effective field in the channel falls also, primarily because the

**Table 2. Measured VPP Across the Microsystem at Various Frequencies and Carrier Ionic Strengths<sup>a</sup>**

$f$ (Hz)	DI water pH 6.9		5 $\mu$ M buffer pH 7.5		50 $\mu$ M buffer pH 8.2		500 $\mu$ M buffer pH 8.6		5 mM buffer pH 8.9	
	VPP (V)	fraction VPP	VPP (V)	fraction VPP	VPP (V)	fraction VPP	VPP (V)	fraction VPP	VPP (V)	fraction VPP
1	1.99	0.995	1.98	0.99	1.98	0.99	1.98	0.99	1.98	0.99
5	1.98	0.99	1.95	0.975	1.92	0.96	1.89	0.945	1.92	0.96
10	1.93	0.965	1.85	0.925	1.86	0.93	1.88	0.94	1.87	0.935
50	1.92	0.96	1.72	0.86	1.67	0.835	1.66	0.83	1.53	0.765
100	1.91	0.95	1.6	0.8	1.56	0.78	1.51	0.755	1.29	0.645
200	1.90	0.945	1.49	0.745	1.45	0.725	1.35	0.675	1.03	0.515

<sup>a</sup> The applied voltage was 2.0 VPP, and carrier flow rate 1.0 mL/h. Source resistance of the power supply was 60  $\Omega$ .

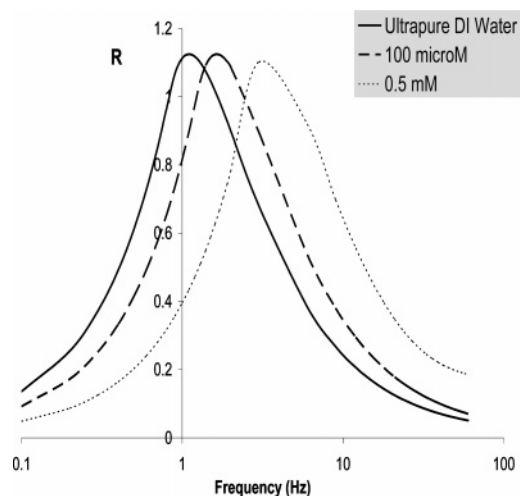


**Figure 4.** Modeled  $R$  values for various ionic strengths using the lumped electrical parameter model. The applied voltage is 3 VPP with flow rate 1.0 mL/h; mobilities were approximately 70, 80, and 88% of  $2.57 \times 10^{-4} \text{ cm s}^{-1} \text{ V}^{-1}$  for DI water, 100  $\mu\text{M}$ , and 0.5 mM ionic strengths, respectively. Results from Table 1 are used to determine the magnitude of the bulk electric field.

double layer capacitance values increase with increasing ionic strength (Table 1).

In earlier work, Palkar and Schure<sup>9,10</sup> showed that the field strengths across the bulk of an EIFFF channel are usually proportional to the product of dc currents and the solution or bulk resistance. When the carrier ionic strength is increased, the bulk resistance goes down and the current in the circuit increases due to the additional ions present for carrying current. However, according to Palkar, the current in the circuit does not increase by the same amount as the bulk resistance decreases with increasing ionic strength, and hence, the voltage across the bulk carrier falls as the carrier ionic strength is increased. Thus, higher currents associated with ionic strength increases do not indicate higher effective fields and, in fact, indicate reduced retention ability in EIFFF. This finding is essentially corroborated in this study for CyEIFFF systems.

Based on the measured lumped electrical parameters of the CyEIFFF system at various ionic strengths and accounting for changes in mobility (using eq 7, the performance of the CyEIFFF microsystem in terms of retention is simulated and shown in Figure 4). The displacement in retention curve is primarily due to the reduction in available applied voltage due to capacitive effects and electrophoretic mobility-related changes when ionic strength is increased. A description of effects related to the magnitude of the effective electric field follows.

**Effective Electric Field.** Based on the lumped electrical parameter model of CyEIFFF<sup>7</sup> and the measured values of  $R_{\text{DL}}$ ,  $C_{\text{DL}}$ , and  $R_{\text{b}}$ , predictions of the effective electric field were made for various operating conditions. As shown previously,<sup>7</sup> the effective electric field remains nearly constant in the operating range of frequencies (0.1–70 Hz) of this work for a fixed ionic strength of the carrier (see Figure 5a). Using the values from Table 1 and eq 5, the effective fields for different carrier compositions were estimated and are shown in Figure 5b. The

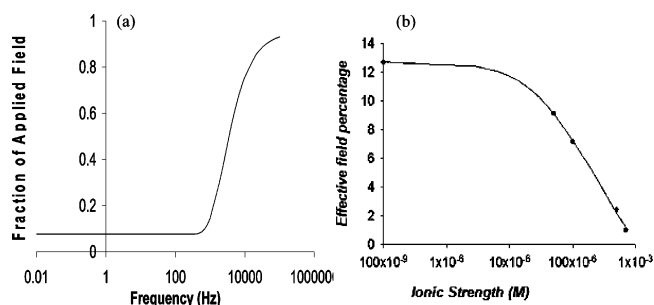


**Figure 5.** (a) Simulation plot showing the effective electric field for a range of frequencies for a CyEIFFF microsystem with a carrier ionic strength of 50  $\mu\text{M}$ . Note that the field is almost constant up to 300 Hz and then increases rapidly with increasing frequency. (b) Effective electric field calculations based on the lumped electrical parameter model and calculated from data in Table 1. The effective electric field rapidly decreases to a small fraction of the applied nominal field value as the ionic strength is increased. The included curve is an exponential fit to the estimated fields.

variation in the effective field values due to changing bulk parameters is not more than 5% and so error bars are not shown.

It is well known<sup>9,10,18</sup> that, in order to have reliable operation of an EIFFF system, the dielectric nature of the bulk phase must not be compromised. For example, the calculated voltage fraction across the bulk at an ionic strength of 5 mM is  $1.5 \times 10^{-3}$  or 0.15% of the applied value. This small field value is similar to or less than the estimated effective electric field in normal (dc) EIFFF systems with low ionic strength carriers and is probably not sufficient to generate any selectivity in retention unless very high voltages (with very high currents) are applied. Thus, at very high carrier ionic strengths, little retention is expected. To verify this assumption, particle retention experiments were carried out as discussed in the next section.

#### CyEIFFF Performance at Various Ionic Strengths and pH.

A particle's electrophoretic mobility is a strong function of the pH of the carrier solution in addition to the dependence on ionic strength.<sup>13,19</sup> An excellent description of ionic strength and pH effects on the electrophoretic mobility of polystyrene particles is given by Elimelech and O'Melia.<sup>20</sup> Elimelech's work suggests that in CyEIFFF the particle elution time should change with varying buffer pH and ionic strength values, but it is not clear if the electrophoretic mobility change is the main driver that outweighs electrical changes.

The results of retention experiments using various ionic strengths for air-equilibrated DI water are plotted in Figure 6. One can observe the particles' elution times decrease as the ionic strength in the buffer was changed from 5 to 50  $\mu\text{M}$ . This change in elution time could be caused by an increase in the electrophoretic mobility of these particles with increasing ionic strength (which would cause a shift to the right), which is consistent with previous observations<sup>21</sup> and eq 7, but is more likely due to the decrease in the effective electric field. In Figure 6, there is a lot of crossover in the elution time curves for 50  $\mu\text{M}$ , 500  $\mu\text{M}$ , and

(17) Loew, E. A.; Bergseth, F. R. *Direct and alternating currents*, 4th ed.; McGraw-Hill Book Co. Ltd.: New York, 1954.

(18) Caldwell, K. D.; Gao, Y. S. *Anal. Chem.* **1993**, *65*, 1764–1772.

(19) Chen, S. B.; Keh, H. J. Boundary effects and particle interactions in electrophoresis. In *Interfacial forces and fields: Theory and applications*; Hsu, J. P., Ed.; Marcel Dekker: New York, 1999.

(20) Elimelech, M.; O'Melia, C. R. *Colloids Surf* **1990**, *44*, 165–178.

(21) Hunter, R. H. *Zeta potential in colloid science: Principles and applications*; Academic Press: London, 1981.

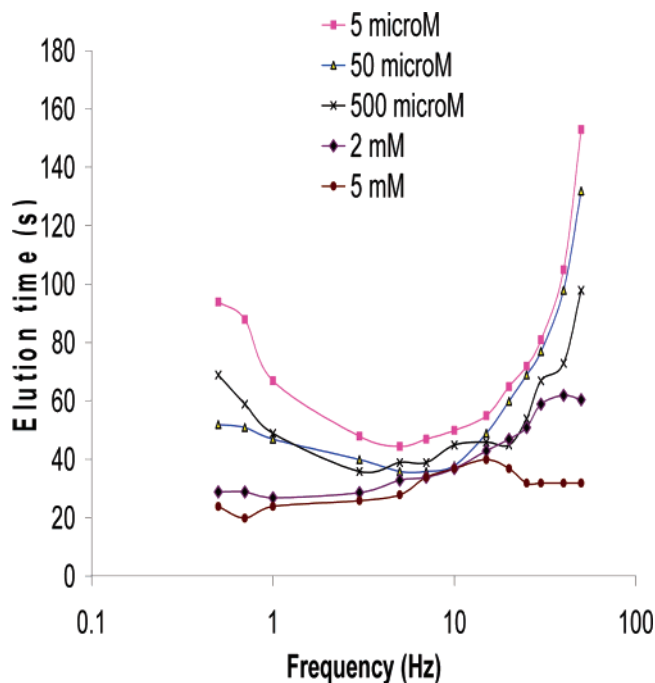


**Figure 6.** Elution times from microscale CyEIFFF experiments with aminated 100-nm PS nanoparticles in various ionic strengths of ammonium carbonate in air equilibrated DI water. The applied voltage was 5.0 VPP with a carrier flow rate of 1.0 mL/h (stop flow relaxation). The retention in general goes down as the ionic strength is increased.

2.0 mM suggesting the possibility of two countereffects going on in the system: one, where electrophoretic mobility changes with increasing ionic strength (goes through a maximum), and the other, where the electric field decreases. At a relatively high ionic strength of 5.0 mM (from the perspective of EIFFF systems), the retention of particles is very low and is almost constant for all the frequencies, indicating that the field experienced by the particles is very low and probably not sufficient for useful operation. Similar trends were obtained using carrier solutions at higher ionic strengths. Injected particles were practically unaffected or unretained in the nearly absent electric field caused by high double layer polarization and elute out at the void time or a short time later.

The crossover in elution times shown in Figure 6 for higher carrier ionic strengths may potentially be explained by changes to the mobility. As described by Elimelech and O'Melia,<sup>20</sup> the electrophoretic mobility of polystyrene particles increases when the ionic strength is increased (from zero to  $\sim 1.0$  mM), reaches a maximum, and then decreases for higher strengths (higher than 1.0 mM). Similar accounts for such an increase in the surface potential at lower ionic strengths ( $\sim 10^{-6}$ – $10^{-3}$  M) for polystyrene nanoparticles are provided in the literature.<sup>22–26</sup> The fact that there is some crossover in the elution times (at 500  $\mu$ M and 2.0 mM)

(22) Folkersma, R.; van Diemen, A. J. G.; Stein, H. N. *Langmuir* **1998**, *14* (21).

(23) Boe, U.; Scheler, U. *Colloids Surf., A: Physicochem Eng. Aspects* **2003**, *222*, 35–40.

(24) Booth, F. *Proc. R. Soc. London* **1950A**, *203*, 514.

(25) O'Brien, R. W.; White, L. R. *J. Chem. Soc., Faraday Trans. 2* **1978**, *74*, 1607.

(26) Caldwell, K. D. Electrical field-flow fractionation. In *Field-flow fractionation handbook*; Schimpf, M., Caldwell, K., Giddings, J. C., Eds.; John Wiley and Sons Inc.: New York, 2000.

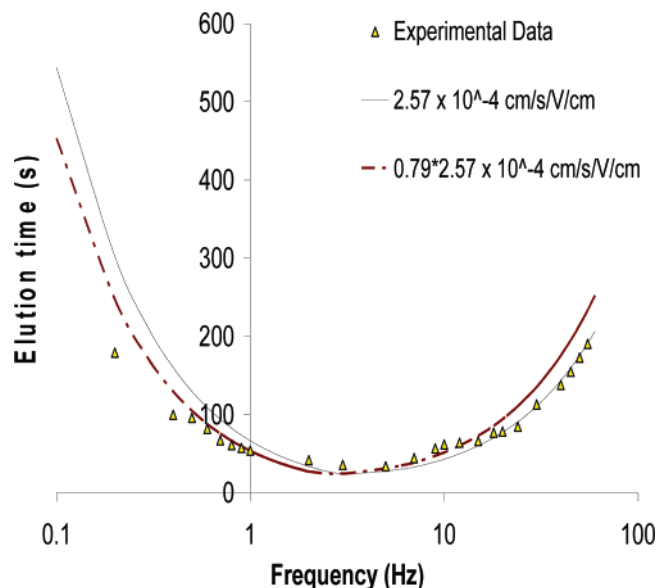


**Figure 7.** Comparison of modeled and experimental data. The calculated elution times represented by the curves are evaluated using the respective mobility values as shown on the plot from the lumped electrical parameter model for a 100  $\mu$ M ionic strength carrier. The applied voltage was 3.0 VPP square waveform, and the flow rate was 1.0 mL/h. The measured mobility was  $2.57 \times 10^{-4} \text{ cm s}^{-1} \text{ V}^{-1} \text{ cm}^{-1}$  at pH 8.84. The adjusted mobility using eq 7 was only 79% of the measured mobility or  $2.03 \times 10^{-4} \text{ cm s}^{-1} \text{ V}^{-1} \text{ cm}^{-1}$ .

indicates that the electrophoretic mobility values may be going through maximums in their mobility values.

To determine the role played by changes in the electrophoretic mobility of the particle relative to the electrical lumped parameter values, experimental data for a 100  $\mu$ M carrier solution were obtained from retention experiments and are shown in Figure 7. Figure 7 shows that the computed values from the lumped electrical parameter model<sup>7,8</sup> using the adjusted (for ionic strength) electrophoretic mobility (i.e.,  $2.03 \times 10^{-4} \text{ cm s}^{-1} \text{ V}^{-1} \text{ cm}^{-1}$ ) value show the best fit to the experimental data at low frequencies (below 5 Hz). Above 5 Hz, the higher electrophoretic mobility ( $2.57 \times 10^{-4} \text{ cm s}^{-1} \text{ V}^{-1} \text{ cm}^{-1}$ ) value shows a better fit. In any event, both mobility values show reasonable fits, which means that it is not clear that electrophoretic mobility changes with ionic strength are significant enough to be concerned with for most experiments.

The results for experiments at various pH values (at the same base concentration of 50  $\mu$ M ammonium carbonate in DI water) are plotted in Figure 8. From pH 8.01 to 8.89, a decrease in the retention time of the particles was observed as the pH values were increased. This result supports an increase in the electrophoretic mobility as predicted by eq 7 but suggests that the electrical effects in terms of the lumped electrical parameter model may be small.

Since overall conductivity of the carrier, and not just ionic strength, is very important in determining the retention, the results of retention experiments with aminated 100-nm PS particles in an ultrapure DI water carrier (at 1.0 mL/h) with a 3.0 VPP applied square waveform are presented in Figure 9. One may observe that, as the conductivity of the carrier solution was increased, there was a drop in the retention consistently. For a constant frequency, the retention time values decreased with increasing conductivity of the carrier solutions. At higher conductivities, the retention was

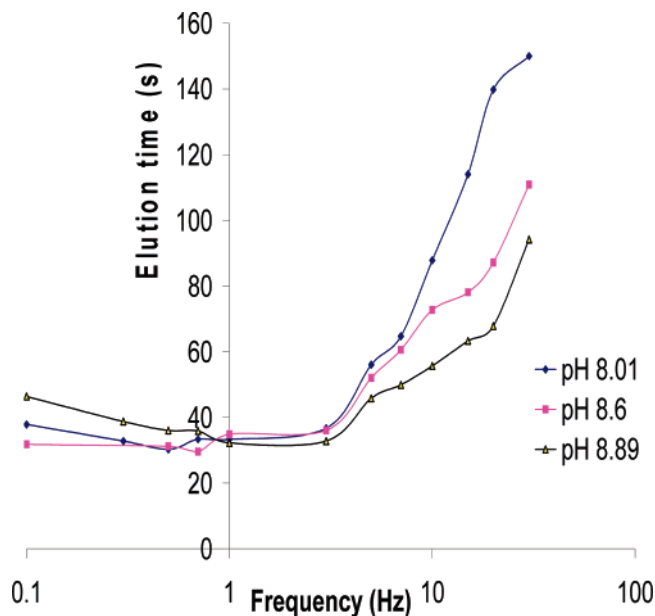


**Figure 8.** Effect of pH conditions on particle retention in CyEIFFF. The ammonium carbonate base concentration was 50  $\mu\text{M}$  in air-equilibrated DI water. The pH of air-equilibrated DI water was varied using potassium hydroxide and hydrochloric acid. The applied voltage was 3.0 VPP square wave, with a carrier flow rate of 1.0 mL/h with stop flow relaxation.

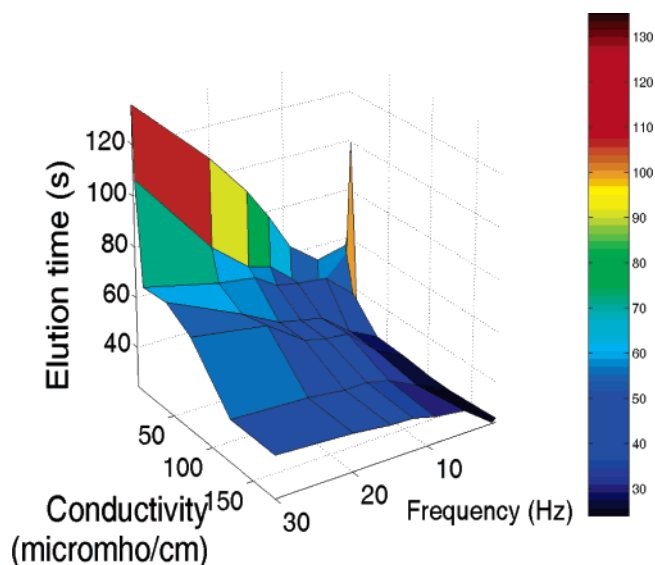


**Figure 9.** Surface plot for particle elution times (experimental data values) as a function of frequency and conductivity of the carrier. The results are obtained with aminated 100-nm PS nanoparticles for carriers flowing at 1.0 mL/h. The applied voltage was a 3.0 VPP square waveform.

nearly constant and small. Figure 9 reiterates the need for using low-conductivity solutions to increase retention.

**Peak-Broadening Effects Based on Plate Height Calculations.** The result of plate height measurements is shown in Figure 10 for several carrier conductivity conditions. Usually, a smaller value of plate height is preferable and gives a quantitative measurement of the extent of peak broadening. Observing the results presented in Figure 10 for CyEIFFF, the plate height and peak broadening increases with increasing carrier ionic strength. Also, it is evident that peak broadening is low near the transition

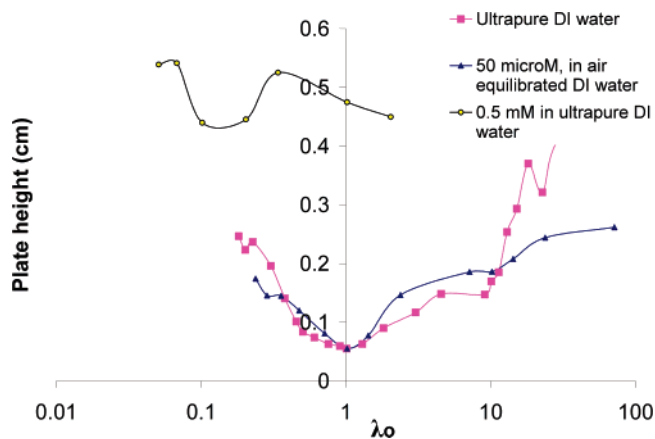


**Figure 10.** Peak-broadening effects characterized using plate height calculations. The experiments were performed using 3.0 VPP and a 1.0 mL/h carrier flow rate. While calculating retention parameters, electrophoretic mobilities were adjusted using eq 7 for various ionic strengths. The values of retention parameter ( $\lambda_0$ ) were calculated using the bulk electrical parameter values (see Table 1) and eq 5.

frequencies ( $\lambda_0 = 1$ ) and increases away from the transition point, which seems to suggest that peak broadening is associated with retention in the channel. The proposed reason for this effect is that, since time is associated with dispersion, and CyFFF does not rely on equilibrium processes, as normal FFF does, the longer particles remain in the channel, the greater peak broadening becomes. This explanation suggests that high carrier velocities will be needed to reduce broadening during high retention analyses.<sup>8</sup> Interestingly, for high ionic strength carriers, even with short retention times, the plate heights are large and constant suggesting that random processes begin to take over and the applied field plays either a minimal role or a dispersive role in the motion of the particles. Unfortunately, these results suggest that CyEIFFF will not perform well in higher ionic strength conditions unless other means are used to combat the loss in effective field (e.g., redox couples<sup>9,27</sup>).

Another potential cause of peak broadening with increasing carrier ionic strength is associated with an increase in carrier conductivity. As the conductivity is increased, the particles' and electrodes' double layers get thinner. As shown by Hao et al.,<sup>19</sup> the particle mobility is altered locally in the case of thinner double layers, when the particle approaches the wall. For such an event, when the sign of the wall charge is same as that on particle, the particle motion is assisted, while it is impeded when the charge is opposite. In the context of CyEIFFF, locally enhanced mobility may push the polystyrene particle further away toward the faster flow lines before the cycle reverses polarity allowing them to elute out sooner. This electrophoretic boundary effect may be important as conductivity increases and may explain why the elution times drop as the conductivity is increased. The modeling of this phenomenon is beyond the scope of this work.

**Failure of the Lumped Electrical Parameter Model: Possible Causes and Suggested Work.** The lumped electrical parameter model for predicting the effective field in CyEIFFF<sup>7,8</sup> does not impose any constraints related to experimental conditions on the applicability of the model itself. The overall lack of

(27) Bard, A. J.; Faulkner, L. R. *Electrochemical methods: Fundamentals and applications*, 2nd ed.; John Wiley & Sons: New York, 2001.

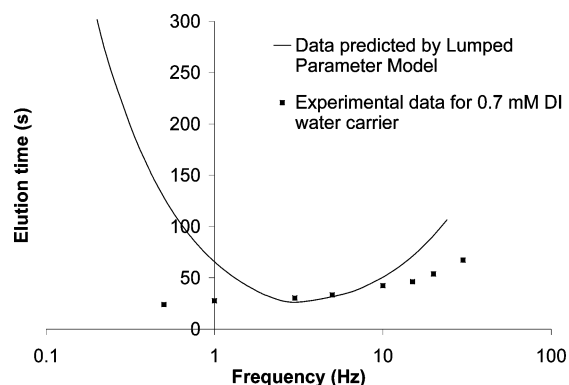


**Figure 11.** Failure of the lumped electrical parameter model<sup>7,8</sup> when the carrier ionic strength was increased to 0.7 mM. The model subsequently failed to predict elution times for all higher ionic strengths. The flow rate was set at 1.0 mL/h, and the applied voltage was a 3.0 VPP square waveform. The mobility was  $2.57 \times 10^{-4} \text{ cm s}^{-1} \text{ V}^{-1} \text{ cm}^{-1}$ , which was adjusted to 88% of its value, i.e.,  $2.26 \times 10^{-4} \text{ cm s}^{-1} \text{ V}^{-1} \text{ cm}^{-1}$  using eq 7.

generality of the model becomes apparent when comparing experimental data using a 0.7 mM ionic strength carrier with the modeled results. The model failed to predict the performance as seen in Figure 11. The results of the model were in good agreement with the experimental data up until the carrier ionic strength was 0.5 mM; however, beyond 0.5 mM there was a severe discrepancy. Because of this poor agreement between the model and experiment, the field computations for carrier ionic strengths above 0.5 mM were considered not useful and, therefore, are not given in this paper.

The reasons for model failure for carrier ionic strengths above 0.5 mM could be many. First, the model takes experimental lumped electrical parameter data and computes the bulk field and particle retentions. At higher ionic strengths, the bulk field may become extremely low. Mathematically, the model calculations are unaffected by this small number; however, experimentally the particles do not experience enough effective electric field to overcome dispersive effects such as diffusion and advection. Second, particle interaction and double layer effects may become significant along with intraparticle interactions (such as repulsion,

local conductivity changes on particle surfaces, and wall repulsion effects). The CyFFF theory is based on the motion of a single particle, whereas the reality is that there are numerous particles and their interactions<sup>19</sup> may play a role in increasing dispersion. Dispersive interactions with the wall may also increase.<sup>28–30</sup> Future efforts may be required to better understand these effects.

Finally, it is quite possible that, for other chemistries and carrier solution properties, the double layer properties may be different giving rise to unique failure modes; hence, care should be exercised in using the lumped electrical parameter model to calculate effective fields for experiments using higher conductivity solutions.

## CONCLUSION

Much consideration was given in this work to the analysis of electrical parameters of the CyEIFFF microsystem at various ionic strength conditions, and various electrical effects in CyEIFFF microsystems were explained. The previously proposed lumped electrical parameter model for calculating effective fields assumes constant double layer electrical properties, which was found not to be the case when the ionic strength or pH of the carrier changes. An increase in carrier ionic strength was found to cause a decrease in effective field available for retaining particles and above  $\sim 1.0$  mM, little retention was observed. Retention was shown to be a strong and sensitive function of the carrier conductivity, and it was shown that with increasing carrier conductivity particle retention decreases. Plate heights in CyEIFFF were also shown to increase with carrier ionic strength. The nature and magnitude of the effective electric field was determined in for a variety of carrier ionic strengths and conditions, and the lumped electrical parameter model for calculating the effective field in the channel was found to be good for carrier ionic strengths up to  $\sim 0.5$  mM. The success and failure modes of the mathematical model were outlined. Overall, microscale CyEIFFF systems were found to perform poorly during higher carrier ionic strength conditions, because retention and effective field fall, while peak broadening increases. But the same systems were found to perform well in low ionic strength conditions and may find application in analyzing and characterizing nanoparticles amenable to these conditions,

Received for review December 4, 2005. Accepted February 3, 2006.

AC0521271

(28) Williams, P. S.; Koch, T.; Giddings, J. C. *Chem. Eng. Commun.* **1992**, *111*, 121–147.

(29) Williams, P. S.; Xu, Y.; Reschiglian, P.; Giddings, J. C. *Anal. Chem.* **1997**, *69*, 349–360.

(30) Goldman, A. J.; Cox, R. G.; Brenner, H. *Chem. Eng. Sci.* **1967**, *22*, 653–660.